Structural Design Optimization of the Turbine Baffle Based on the Slime Mould Algorithm of Zhizhou Software

PEI Ben[1], *LIU Yiyuan*[2], *CHEN Yalong*[2,3], *TENG Da*[1], *HOU Naixian*[2], *MI Dong*[4], *YAN Cheng*[1*]

1. School of Aerospace Engineering, Xiamen University, Xiamen 361102, P. R. China; 2. AECC Commercial Aircraft Engine Co., Ltd, Shanghai 200241, P. R. China; 3. School of Mechanical and Power Engineering, East China University of Science & Technology, Shanghai 200237, P. R. China; 4. Hunan Aviation Powerplant Research Institute, Aero Engine Corporation of China, Zhuzhou 412002, P. R. China

(Received 29 September 2025; revised 10 February 2026; accepted 1 March 2026)

Abstract: As a critical component of the turbine rotor, the baffle plays an essential role in ensuring safe and reliable operation of the aero-engine. This study addresses the issue of excessive local stress in the baffle of a high-pressure turbine disc. The structural design optimization is performed using the self-developed Zhizhou software integrated with the slime mould algorithm (SMA). Leveraging advanced algorithms and comprehensive simulation interfaces, the Zhizhou software effectively exploits the potential of structural design, leading to significant improvements in structural performance. The SMA algorithm employs a positive feedback mechanism and adaptive strategies through the incorporation of fitness weights and oscillation factors. These parameters simulate the oscillatory contraction behavior of slime moulds, allowing the algorithm to dynamically adjust search direction and speed, thereby achieving an effective balance between local exploration and global optimization. During the optimization process, a sector sub-model is established, and the contact model is simplified using a force load equivalence approach to improve computational efficiency. Subsequently, a parametric model of the baffle is developed based on geometric characteristics, stress responses, and boundary constraints, with the variation ranges of key parameters being determined. A mathematical model is then formulated with the objective of minimizing the maximum equivalent stress, under the constraint of the axial support reaction force at the contact surface. Finally, an integrated design optimization workflow is constructed using Zhizhou in combination with Unigraphics (UG) and Workbenchs, as well as incorporating the SMA algorithm to optimize the baffle structure. After optimization, the maximum equivalent stress is decreased from 1 382.4 to 1 235.4 MPa, a reduction of 10.6%. Meanwhile, the axial support reaction force is increased from 4 158.9 to 4 330.6 N, a variation of 4.0%, which satisfies the requirement for being within 12%. These results validate the effectiveness of the SMA algorithm in the structural design optimization of the baffle and demonstrate the practical value of the Zhizhou software in engineering applications.

Key words: high-pressure turbine; baffle; Zhizhou software; slime mould algorithm (SMA); structural optimization

CLC number: V232 **Document code:** A **Article ID:** 1005-1120(2026)03-0412-15

0 Introduction

As a core component of an aero-engine, the turbine rotor must be designed with high stability and reliability to ensure operational safety. The baffle, a critical part of the turbine rotor, serves to restrict the axial movement of turbine blades and form cooling airflow channels[1]. Due to its harsh operating environment, the baffle is subjected to significant centrifugal forces and thermal stresses[2], and susceptible to stress concentration and potential fatigue failures[3]. Therefore, reducing the stress concentration of the baffle is crucial to the safe and stable operation of the engine.

*Corresponding author, E-mail address: yanchengmail@xmu.edu.cn.

How to cite this article: PEI Ben, LIU Yiyuan, CHEN Yalong, et al. Structural design optimization of the turbine baffle based on the slime mould algorithm of Zhizhou software[J]. Transactions of Nanjing University of Aeronautics and Astronautics, 2026, 43(3): 412-426.

http://dx.doi.org/10.16356/j.1005-1120.2026.03.007

Currently, research on turbine rotor baffles primarily focuses on stress analysis, whereas studies on stress optimization remain relatively scarce and are predominantly conducted by traditional optimization algorithms. For example, Meng et al.[4] conducted computational analysis on the centrifugal stress of boltless baffles in aero-engines. They used a sector sub-model to study the stress distribution of the baffle under different rotational speeds and found that stress concentration mainly occured in the fillet area near the contact surface. Luan et al.[5] conducted a finite element analysis on a boltless baffle, with a focus on the contact pressure between the baffle and the blades. Their study established the relationship among rotational speed, the gas pressure difference across the baffle, and the resultant pressure provided by the boltless baffle. Zeng et al.[6] optimized the baffle bolt holes using sub-model analysis technology, resulting in a 13.8% reduction in the maximum equivalent stress after optimization. Song et al.[7] carried out shape optimization on the turbine disk baffle structure based on mesh deformation technology and using a gradient algorithm, which reduced the first principal stress of the sealing disk by 13.6% after optimization.

With the rapid development of swarm intelligence algorithms such as genetic algorithms and particle swarm optimization algorithms, structural optimization can efficiently adjust design parameters and more accurately control stresses in key areas, thereby significantly improving structural performance[8]. These algorithms have been widely applied to the design of aero-engine turbine structures. For example, Yang et al.[9] carried out structural optimization design on turbine tenons and mortises using the multi-island genetic algorithm and the sequential quadratic programming algorithm. After optimization, the maximum equivalent stress of the tenon was reduced by 29.5%, and that of the mortise by 32.5%. Zhang et al.[10] developed an aero-engine turbine stator structural optimization design system based on the genetic algorithm. Through optimizing the turbine stator, the maximum equivalent stress around the holes was reduced by 20.7%, significantly improving the comprehensive performance of the structure. Sivashanmugam et al.[11] optimized the axial flow turbine using the multi-objective genetic algorithm, which reduced the maximum equivalent stress by 50% and increased the stage efficiency by 0.8%, effectively improving the engine performance.

Although structural optimization has been widely applied to the design optimization of typical turbine structural components, scholars usually conduct relevant research using foreign engineering optimization software such as Isight. For example, Song[12] used Isight and combined it with the secondary development technology of software like Patran and Nastran to build an automated solution platform for turbine disk structural optimization, and verified its effectiveness in turbine disk optimization. In addition, Fan et al.[13], Shangguan et al.[14], and others also conducted optimization studies on turbine blade shrouds using Isight software. However, foreign commercial software has significant shortcomings in compatibility and customized services, especially in supporting interfaces of domestic software. Their closed architecture results in limited flexibility in customized services, making it difficult to meet the in-depth needs of specific engineering scenarios. Foreign software also has obvious limitations in algorithm integration. Taking Isight as an example, it has built in more than 20 optimization algorithms, mainly traditional gradient algorithms, supplemented by basic optimization methods such as genetic algorithms and particle swarm optimization algorithms as well as their traditional improved versions. Such an algorithm library is difficult to meet the needs of modern engineering optimization, especially unable to effectively integrate emerging meta-heuristic intelligent and efficient optimization algorithms, and often performs poorly in solving high-dimensional nonlinear problems. This lack of advanced algorithms further limits its application effect in complex engineering optimization. Therefore, the development of self-developed domestic software can make up for the shortcomings of existing tools and better meet domestic engineering needs, providing strong support for the design of key models.

In summary, current research on the structural optimization of turbine rotor baffles is relatively limited, and the potential of structural performance has not been deeply explored by combining high-performance software and advanced intelligent optimization algorithms. In addition, traditional foreign engineering software provides limited support for the design of key models. Therefore, it is necessary to develop domestic high-performance software, integrate tools such as computer aided design (CAD) and computer aided engineering (CAE), and carry out research on the structural design optimization of baffles based on advanced intelligent algorithms. The slime mould algorithm (SMA) has the characteristics of few parameters, strong optimization ability, and excellent convergence performance[15]. Therefore, aiming at the problem of excessive local stress in the baffle of the high-pressure turbine disk of an areo-engine, this paper constructs a design optimization process combining Unigraphics (UG) and Workbench based on the self-developed Zhizhou software, and integrates the SMA algorithm to carry out the structural design optimization of the baffle.

1 Optimization Software and Algorithm

1.1 Zhizhou software

Zhizhou is a multidisciplinary and multi-objective shape and topology design optimization platform jointly developed by Aero Engine Corporation of China (AECC) Commercial Aircraft Engine Co., Ltd., Hunan Aviation Powerplant Research Institute, and Xiamen University. It aims to help break through key technologies in the development of complex equipment such as aero-engines and enhance technological innovation capabilities[16].

Zhizhou integrates a variety of optimization algorithms, including not only traditional optimization algorithms such as mathematical programming methods and gradient algorithms, but also dozens of intelligent optimization algorithms developed and tested for complex engineering problems, such as meta-heuristic optimization algorithms like SMA[15] and the whale optimization algorithm[17], as well as stochastic optimization algorithms such as the adaptive simulated annealing[18]. In addition, the software also integrates advanced experimental design algorithms including Latin hypercube sampling[19] and full factorial design[20], as well as high-precision surrogate models such as support vector machines[21] and Kriging[22]. These algorithms and models can effectively balance index conflicts in multidisciplinary design and achieve the optimal comprehensive performance of the system. Combined with intelligent algorithms, the software can optimize the shape and structure of complex equipment, and comprehensively coordinate the design requirements of multiple disciplines such as aerodynamics, combustion, heat transfer, and strength, thereby realizing lightweight and high-performance structural design while meeting multidisciplinary requirements.

As shown in Fig.1, relying on a complete set of simulation software interfaces, the Zhizhou software can seamlessly connect with common engineering simulation tools (such as commercial software including ABAQUS, ANSYS, CFX, and UG), realizing the close integration of optimization algorithms with practical engineering problems. It can be widely applied to various fields such as aero-engines and mechanical equipment.

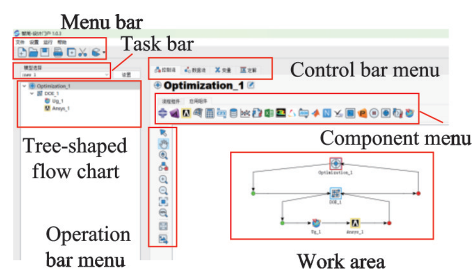

Fig.1 Schematic diagram of Zhizhou software

1.2 Slime mould algorithm

SMA is a meta-heuristic algorithm that simulates the food-seeking process of slime mould. Veins form between the slime mould and food sources; when veins approach food sources, bio-oscillator produces propagating waves[23], increasing cytoplasmic flow through the veins. The faster the flow, the thicker the veins. Through the combination of positive and negative feedback, the slime mould can establish an optimal path to food in a relatively superior manner[24].

The core idea of SMA is to simulate the movement of slime mould individuals through position updates. The algorithm achieves multi-angle search using random functions and dynamically adjusts the movement direction of individuals by simulating the positive feedback mechanism of the slime mould with weight coefficients. Random parameters simulate the uncertainty of slime mould vein contraction patterns, enhancing search randomness. Meanwhile, the algorithm introduces oscillation factors to simulate the selection behavior of the slime mould. Thus, it oscillates within a certain range and gradually approach 0 as the number of iterations increases. This realizes a smooth transition from global exploration to local exploitation. By combining positive feedback mechanisms and adaptive strategies, SMA simulates the oscillatory contraction behavior of the slime mould through fitness weight coefficients and oscillation factors, dynamically adjusts the search mode, and effectively balances local exploration and global optimization capabilities.

The flow chart of the SMA optimization algorithm is shown in Fig.2, with the specific steps as follows.

(1) Initialize population and calculate fitness. The fitness value is calculated by evaluating the position of each individual, with higher values indicating closer proximity to the optimization objective.

(2) Calculate the weight coefficient of each individual according to the fitness value. The mathematical formula for the weight coefficient W is

$$\begin{cases} W(S_r(i))=\begin{cases} 1+r\cdot\log\left(\dfrac{F_b-S(i)}{F_b-F_w}+1\right) & \text{Condition} \\ 1-r\cdot\log\left(\dfrac{F_b-S(i)}{F_b-F_w}+1\right) & \text{Others} \end{cases} \\ S_r=\text{sort}(S) \end{cases} \tag{1}$$

where "condition" indicates that the fitness value $S(i)$ ranks in the first half of the population; r a random value within [0, 1]; F_b the best fitness obtained in the current iteration; F_w the worst fitness obtained in the current iteration; S_r the ascending sequence of fitness values for the minimization problem.

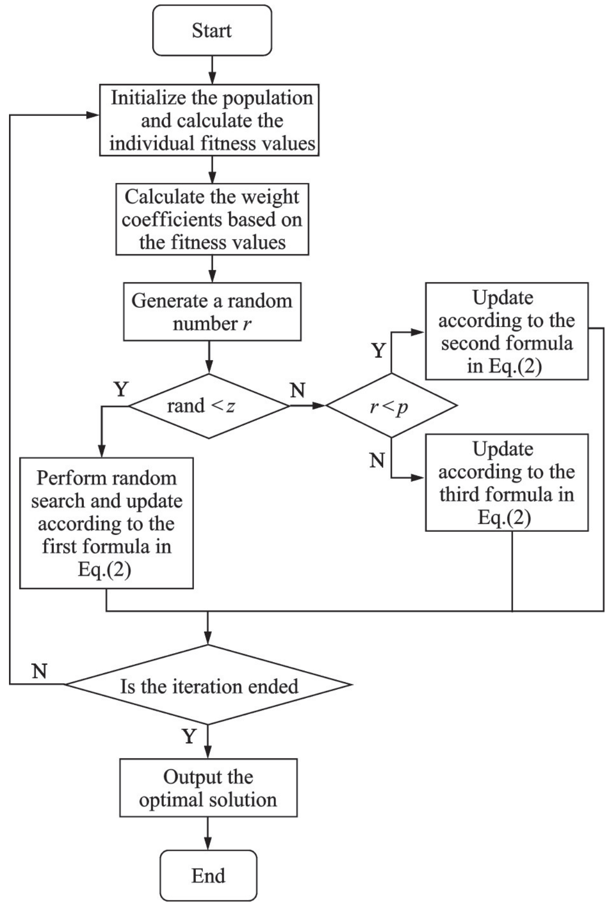

Fig.2 Schematic diagram of SMA optimization process

(3) Update the position of each individual according to the position update formula. The position update formula of the SMA algorithm is

$$X(t+1)=\begin{cases} \text{rand}\cdot(B_U-B_L)+B_L & \text{rand}<z \\ X_b(t)+v_b\cdot(W\cdot X_A(t)-X_B(t)) & r<p \\ v_c\cdot X(t) & r\geqslant p \end{cases} \tag{2}$$

where B_L and B_U represent the lower and the upper bounds of the search range; the rand function denotes a random value between [0, 1]; z is generally set to 0.03; X_b indicates the optimal position of the current slime mould individual and X the position of the slime mould individual at the current iteration step; X_A and X_B denote the randomly selected positions of two slime mould individuals; t the current iteration step; v_b is a control parameter ranging from $[-a, a]$, v_c a parameter that decreases linearly from 1 to 0, W the weight of fitness, and r a random value between [0, 1]; and p is obtained through fitness calculation.

In Eq.(2), p denotes a threshold parameter used to balance global exploration and local exploitation; v_b and v_c are oscillation factors for controlling the movement speed of slime mould individuals. Parameters p and v_b are described as

$$p=\tanh|S(i)-F_D| \tag{3}$$

$$v_b=[-a,a] \tag{4}$$

$$a=\operatorname{arctanh}\left(-\left(\frac{t}{t_{\max}}\right)+1\right) \tag{5}$$

where $i\in 1, 2, \cdots, n$; $S(i)$ represents the fitness of X; F_D the best fitness across all iterations; and $t_{\max}$ the maximum number of iterations.

(4) Record the current optimal solution and decide whether the output condition is met. If it is, the iteration terminates; otherwise, repeat the above steps.

2 Model Analysis and Parametric Modeling

2.1 Research object

Fig.3 illustrates the high-pressure turbine rotor model of an aero-engine, comprising key components such as the baffle, the sealing disk, the interstage disk, and turbine blades. The high-pressure turbine rotor is a typical revolving structure, so the overall model can be divided into sector models. Considering the periodic distribution characteristics of the disk's vent holes, the high-pressure turbine rotor model is segmented into a $3/N$ sector model (where N is the total number of blades), as shown in Fig.3(b). Among them, stress concentration is obvious near the baffle's vent slot and fillet. Therefore, it is necessary to carry out research on the structural design optimization of the baffle. The baffle structure is shown in Fig.3(c).

In this study, UG modeling software is used to create a parametric 3D model of the high-vortex rotor. The 3D model is imported into ANSYS Workbench via ANSYS's CAD interface for finite element analysis. Leveraging the macro-command recording function in Workbench, the generated macro-command file was imported into Zhizhou optimization software. Zhizhou then calls the macro-command file by executing Windows batch commands, thereby automating parameter updates, finite element analysis, and output of calculation results.

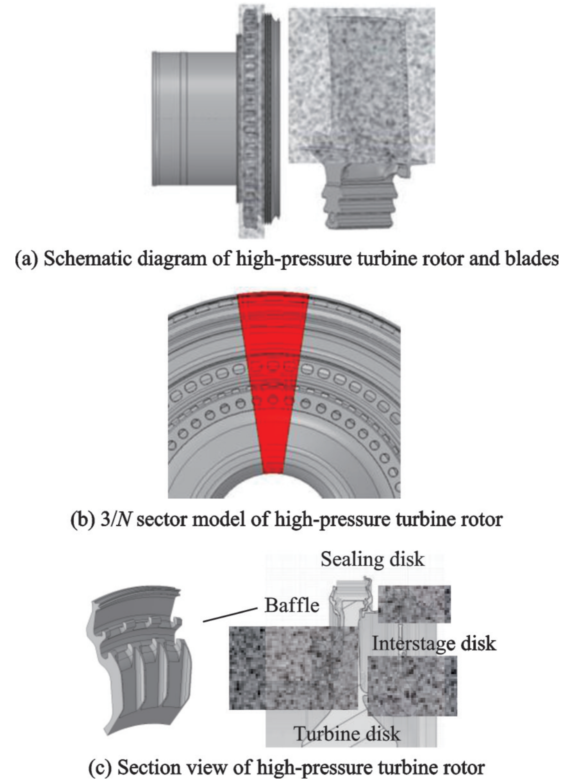

Fig.3 Schematic diagram of high-pressure turbine rotor sector model

2.2 Finite element analysis

For the finite element analysis of complex assemblies, the sub-model analysis technology is usually adopted[25]. The sector model of the high-pressure turbine rotor is further segmented to obtain the high-pressure turbine sub-model. Finite element analysis of the high-pressure turbine sub-model is carried out based on Workbench simulation software. As shown in Fig.4, second-order tetrahedral

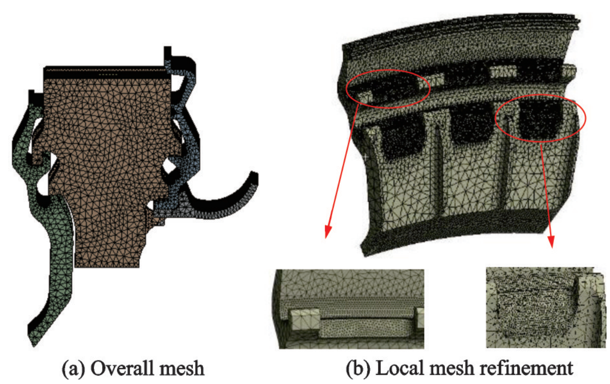

Fig.4 Finite element mesh diagram

mesh elements are used for meshing, with an overall mesh size of 2 mm, and local refinement with a mesh size of 0.5 mm is applied to the key areas of the baffle.

As shown in Fig.5, a finite element model of the high-pressure turbine sub-model is established under a typical operating condition of the engine. The entire high-pressure turbine sub-model is applied with the rotational speed and temperature field corresponding to the typical operating condition, while the pressure difference between the inner and outer surfaces of the baffle and the sealing disk is taken into account. Displacement field constraints need to be imposed on the split surfaces of the baffle, sealing disk, turbine disk, and inter-stage disk. Due to the circumferentially periodic distribution characteristic of the turbine disk, cyclic symmetry constraints must be applied to the circumferential split surfaces of the sub-model.

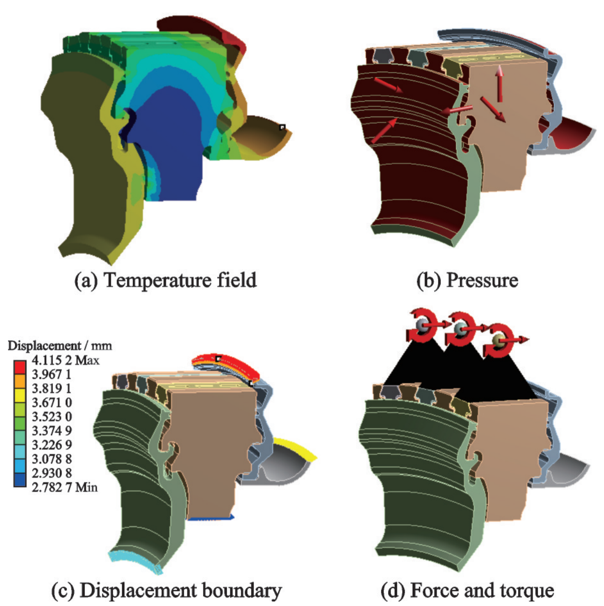

Fig.5 Finite element analysis setup

In addition, due to the segmentation and simplification of the turbine blade, concentrated forces and torques need to be applied at the coupling points on the blade's split surface to equivalently replace the aerodynamic load on the blade, as shown in Fig.5(d). Since the sealing disk is designed to restrict the axial movement of the turbine blade, an interference fit exists between its spigot surface and the blade. Therefore, a displacement field must be applied to the spigot surface of the sealing disk to accurately simulate the actual contact condition between the turbine blade and the baffle.

There are contact relationships between the various components of the sub-model: The baffle, the sealing disk, the turbine disk, the tenon, and the inter-stage disk are all set to frictional contact, while the blade tenon and turbine disk are set to non-separating contact.

Since the sub-model boundary approximates the actual conditions using few applied displacement fields, the accuracy of the resulting calculations is relatively limited. Therefore, the stresses near the displacement boundary and contact boundary are not considered in the analysis. The calculation results of the baffle of the high-pressure turbine sub-model are shown in Fig.6, with the maximum equivalent stress being 1 382.4 MPa, which occurs in the vent slot and fillet areas.

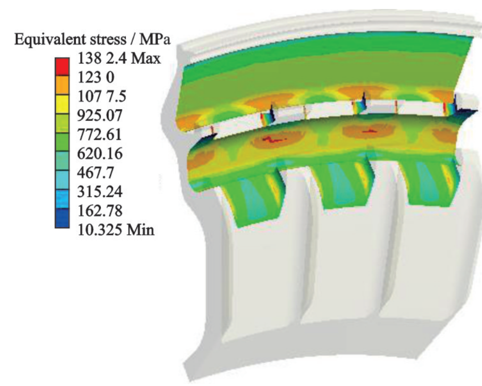

Fig.6 Equivalent stress cloud of the baffle

2.3 Simplification of contact model

When conducting finite element analysis on the high-pressure turbine sub-model, it is found that the computational time is relatively long. To reduce computational time, further model simplification is performed based on this setup. As shown in Fig.7, according to Saint-Venant's principle, the contact relationship between the sealing disk and the inter-stage disk is simplified, and contact force is used to replace the contact mode of the sealing disk. Since the sealing disk restricts the axial movement of the tenon, it is necessary to apply axial displacement constraints on the contact surface of the tenon after simplifying the sealing disk.

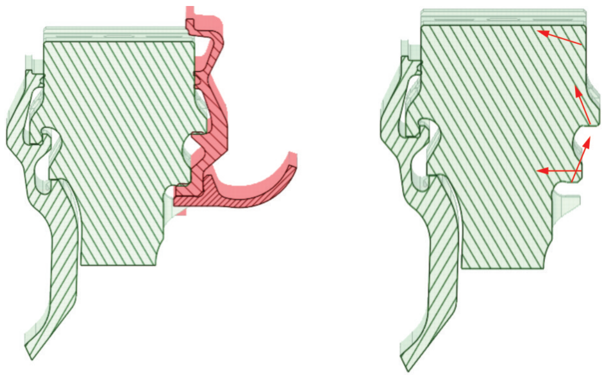

Fig.7 Schematic diagram of contact simplification

To validate the feasibility and effectiveness of this simplified modeling approach, an identical meshing strategy is employed while maintaining consistency in all other boundary conditions. The computer used in the calculation process is equipped with an Intel (R) Xeon (R) Platinum 8 352 V CPU @ 2.10 GHz and 256 GB of RAM. The calculation results of the simplified model are shown in Fig.8 and Table 1. The maximum equivalent stress of the simplified model is 1 378.7 MPa, with an error of approximately 0.3% compared with the calculation result of 1 382.4 MPa of the original sub-model, which meets the requirements of engineering design. Meanwhile, the computation time using frictional contact simplification is about 12 min. Compared with the computation time of the original sub-model (approximately 16 min), the calculation time is reduced by 25%, effectively improving the computation efficiency. Therefore, the aforementioned case validates the feasibility and efficacy of this model simplification approach.

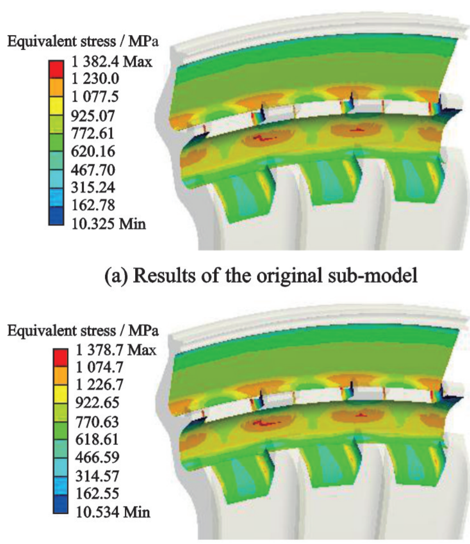

(a) Results of the original sub-model

(b) Results of the simplified model

Fig.8 Comparison of simplified calculation results

Table 1 Comparison of calculation results and time

Model	Maximum stress/MPa	Time of calculation/min
Initial model	1 382.4	16
Simplified model	1 378.7	12
Rate of change/%	−0.3	−25.0

2.4 Model parameterization

Considering the geometric characteristics, stress response, and boundary constraint conditions of the baffle, appropriate parameters are selected to conduct parametric modeling of the baffle. The baffle is a thin-walled structure[26], which bears large centrifugal force and thermal stress, and the curve shape of its cross-section has a significant impact on the structural performance. As shown in Fig.9, there is stress concentration in the fillet area above the baffle, and the stress of the vent slot is also relatively high. Therefore, it is necessary to optimize the wall thickness above the baffle, the fillet, and the shape of the vent slot. The baffle is restricted by assembly constraints and has many contact boundaries, resulting in a small design space, as shown in Fig.9(b).

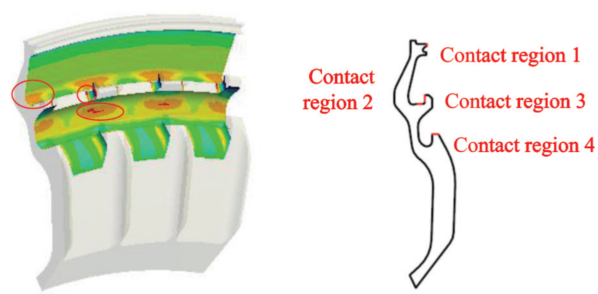

(a) Stress distribution (b) Contact boundary

Fig.9 Stress distribution and contact boundaries

The baffle contains multiple contact surfaces, and these boundary conditions need to be maintained. Therefore, the contact interfaces and their surrounding regions are constrained. As shown in Fig.10, in the parametric modeling process, the design parameters of the baffle are mainly divided into three categories: The wall thickness of the baffle (Fig.10(a)), the fillet dimensions of the baffle

(Fig.10(b)), and the shape control parameters of the vent slots (Fig.10(c)). Since the stress concentration in the fillet area above the baffle is obvious, and the wall thickness directly affects the stress distribution, both the fillet size and the wall thickness of the baffle are included in the design parameters for optimization.

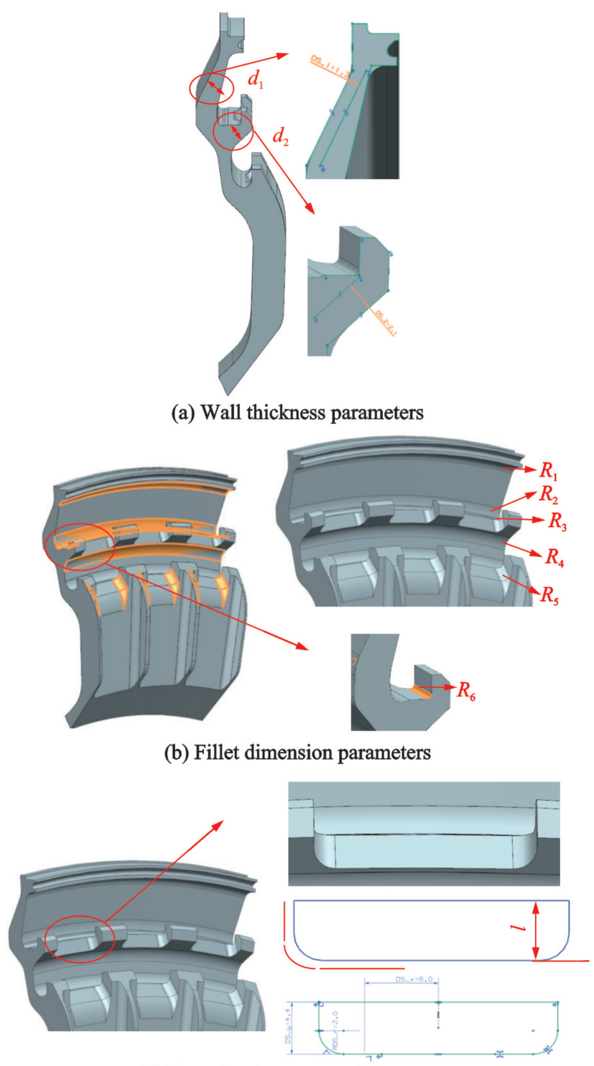

(a) Wall thickness parameters

(b) Fillet dimension parameters

(c) Vent slot shape control parameters

Fig.10 Schematic diagrams of the parameterized model

In addition, the vent slot area of the baffle also has a significant stress concentration problem, requiring optimization and adjustment of its shape. As shown in Fig.10, the vent slot features a racetrack-shaped cross-section, which is geometrically defined by a combination of arcs and straight segments. The vertical distance from the intersection points of these arcs and straight segments to a horizontal reference line serves as a key design parameter, enabling precise control over the final slot geometry. This parametric modeling approach ensures both the continuity of geometric characteristics and facilitates subsequent optimization processes.

As shown in Table 2, in the parametric design of the baffle, the wall thickness includes two independent parameters, whose values directly affect the overall mass of the baffle. To ensure that the mass change is within a reasonable range, it is necessary to set strict upper and lower limit constraints for these two parameters. The setting of fillet parameters and vent slot shape control parameters needs to meet two key conditions: (1) To ensure that the geometric model can be generated normally and avoid modeling failure due to unreasonable parameters; (2) to prevent interference between components. At the same time, any modification to the vent slot geometry must account for its cross-sectional area constraint, since significant deviations in area may adversely affect the cooling performance of the turbine disk. After multiple iterations of validation and refinement, and in consideration of practical manufacturing constraints, the final variation ranges for each parameter are established, as summarized in Table 2.

Table 2 Parameter variation range mm

Parameter	Initial value	Range of variation
d_1	1.25	[0.50, 3.00]
d_2	2.10	[1.00, 5.00]
R_1	2.00	[0.50, 3.50]
R_2	5.20	[0.50, 5.20]
R_3	1.00	[0.50, 4.00]
R_4	4.00	[0.50, 10.00]
R_5	2.00	[0.50, 2.20]
R_6	0.50	[0.50, 1.00]
l	4.44	[4.00, 4.50]

3 Optimization Mathematical Model and Process

3.1 Mathematical model for baffle optimization

The reaction force on the contact surface between the baffle and the tenon is shown in Fig.11. To ensure the baffle's function of axially limiting the blade tenon, it is necessary to control the change of the axial reaction force on the baffle's contact surface within 12% during the optimization process.

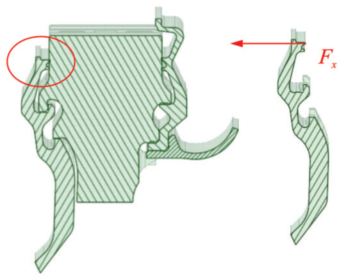

Fig.11 Schematic diagram of the support reaction force at the baffle

Employing the key design parameters of the baffle as design variables, with the minimization of the maximum equivalent stress as the optimization objective and the axial reaction force at the contact surface as the constraint, an optimization mathematical model for the baffle is established. The model can be formulated as

$$\begin{cases} \text{find} & d_i, R_i, l \\ \min & \sigma_{\text{von-Mises max}} \\ \text{s.t.} & F_{\min} \leqslant F_x \leqslant F_{\max} \end{cases} \tag{6}$$

where d_i, R_i, l are the wall thickness, the fillet, and the vent slot shape control parameters of the baffle, respectively; $\sigma_{\text{von-Mises max}}$ is the maximum equivalent stress of the baffle and F_x the axial reaction force of the initial sub-model; $F_{\min}$ and $F_{\max}$ are 88% and 112% of F_x, respectively.

3.2 Establishment of baffle optimization process

As shown in Fig.12, a baffle design and optimization process combining UG and Workbench is established based on the self-developed domestic software Zhizhou, and the structural optimization of the baffle is realized through the following steps.

(1) Update the parametric model. Drive the design parameters through UG to generate an updated geometric model, which serves as an input for subsequent finite element analysis.

(2) Finite element analysis and calculation. Import the updated model into Workbench to perform finite element simulation calculations, and output the calculation results of key performance indicators such as stress and reaction force.

(3) Optimize design parameters using the SMA algorithm. Read the finite element calculation results. The SMA algorithm updates weight coefficients and oscillation factors based on the current fitness value, and dynamically adjusts the search direction and speed.

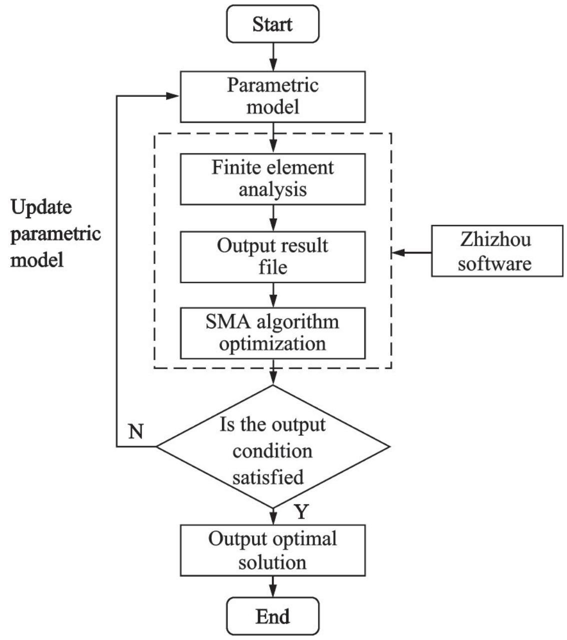

Fig.12 Optimization flow chart of the baffle based on Zhizhou software

(4) Determine whether the output conditions are met. If they are, output the optimal solution; if not, update the design parameters and enter the next iteration.

As shown in Fig.13, an integrated optimization process for the baffle is developed using Zhizhou platform. Zhizhou enables real-time interoperability with applications such as UG and Workbench, facilitating seamless model updates and finite element analysis. Furthermore, Zhizhou supports real-time parameter input and output, and incorporates the SMA algorithm, enabling a fully automated optimization process for the baffle.

Based on previous structural optimization experience, and considering both computational efficiency and optimization performance, the population size is set to 10 and the number of iterations to 100 for the baffle optimization problem. The contraction factor z has a significant impact on the local exploitation and global exploration capabilities of the algorithm, and is set to 0.03 in the baffle optimization, as shown in Table 3.

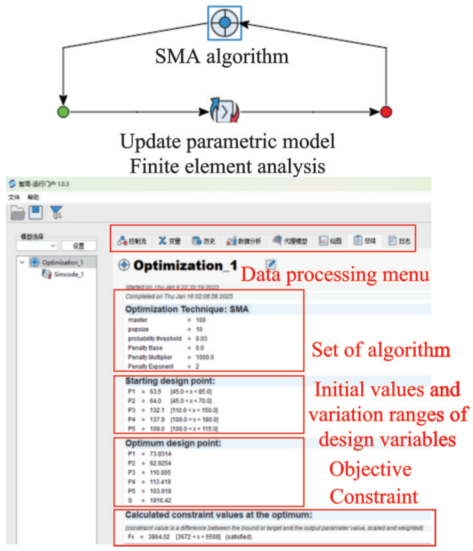

Fig.13 Setup of baffle optimization process on Zhizhou

Table 3 Parameter setup of SMA

Parameter	Population size	Step	Factor
Value	10	100	0.03

4 Analysis and Verification of Optimization Results

The structural optimization process curve of the baffle is shown in Fig.14. A total of 1 000 iterative evaluations are performed during the optimization. In order to increase the probability of finding the optimal solution, the bounds of relevant parameters are set rather aggressively during the parametric modeling of the 3D structure. As a result, some boundary or unconventional parameter combinations lead to model interference, preventing the generation of a valid geometric model. Although these parameters could not guide the optimization direction, the SMA algorithm remained robust and is not significantly disrupted by such data, further demonstrating the reliability of its optimization performance. A total of 10 invalid data sets are generated in this optimization. After removing these invalid data, the optimum solution is obtained at the 958th iteration step.

Fig.14 shows that during the initial phase of optimization, the values on the vertical axis exhibits substantial variations. By leveraging its global exploration mechanism, the SMA algorithm performs extensive searches throughout the parameter space, progressively guiding the solutions toward the target region. As a result, a considerable number of design points generated in this early stage fail to satisfy the prescribed constraints. During the mid-phase of optimization, the algorithm dynamically adjusts its search pattern using oscillation factors and adaptive weight coefficients. This approach effectively prevents convergence to local optima while enabling further refinement through a limited number of exploratory points that escapes local regions. As a result, the amplitude of oscillations in the objective function is significantly reduced. As the optimization is progressing, the number of design points violating the constraints in the later stages is markedly lower than that in the initial phase, demonstrating the algorithm's ability to effectively balance objective pursuit with constraint satisfaction. Ultimately, the algorithm converges consistently and identified the location of the optimal solution.

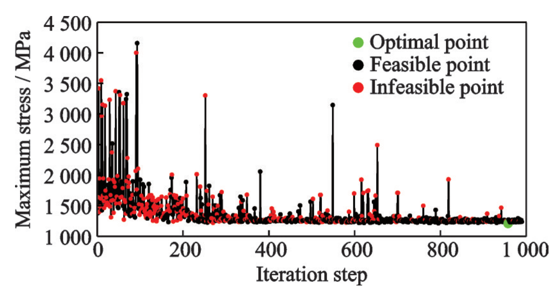

Fig.14 Variation of maximum stress and feasibility distribution during optimization iterations

After optimization, it is necessary to further evaluate the rationality of the optimized structure to avoid interference between models, so the optimization results are subjected to reconstruction verification. Fig.15(a) shows the simplified calculation results of the reconstructed model, with a maximum equivalent stress of 1 234.6 MPa. Fig.15(b) presents the calculation results of the reconstructed model under complete contact conditions, with a maximum equivalent stress of 1 235.4 MPa. The error of the simplified calculation results is approximately 0.06%, which once again verifies the accuracy of the contact model simplification method. Fig.16 presents a comparative analysis of the stress distributions between the optimized configuration and the original model. The maximum equivalent stress in the optimized design measures 1 235.4 MPa, representing a reduction of 10.6% compared to the initial model's value of 1 382.4 MPa.

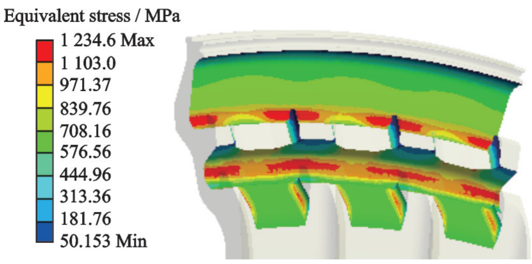

(a) Results of the simplified model after optimization

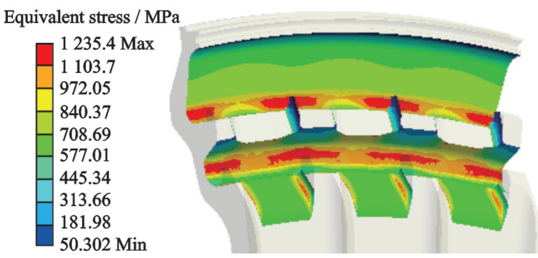

(b) Results of the complete model after optimization

Fig.15 Comparison of stress contours between the simplified model and the complete model after optimization

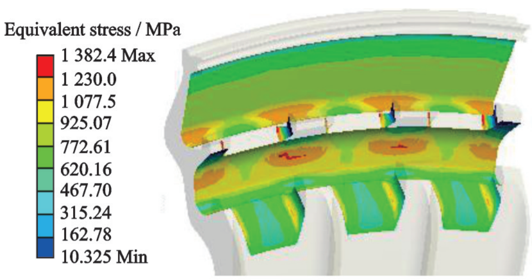

(a) Results of the initial model

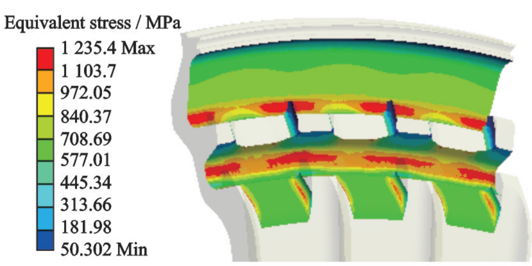

(b) Results of the optimized model

Fig.16 Comparison of equivalent stress contour plots for the baffle before and after optimization

It is necessary to check whether the axial reaction force on the contact surface of the baffle tenon meets the design requirements, and the comparison results are shown in Table 4. The axial reaction force at the contact surface of the initial baffle model is measured at 4 158.9 N, while that of the optimized configuration reaches 4 330.6 N. This corresponds to a variation of 4.0%, well within the design requirement that the change in axial reaction force must remain below 12%.

Table 4 Comparison of calculation results before and after baffle optimization

Model	Maximum stress/MPa	Reaction force/N
Initial model	1 382.4	4 158.9
Optimized mode	1 235.4	4 330.6
Change rate/%	−10.6	+4.0

Table 5 compares the parameter changes before and after optimization. Based on the optimized parameters, the baffle is redesigned as illustrated in Fig.17. In Fig.17, the black solid line depicts the profile of the original baffle model, whereas the red dashed line indicates that of the optimized design. As indicated in Table 5, Figs. 16, 17, the cross-sectional area of the vent slot in the baffle has been reduced. This reduction results from a decrease in the governing shape parameter, which causes the straight segment at the base of the slot to form an angle with the horizontal direction, thereby smoothing the transition at the fillet and effectively mitigating stress concentration in the slot. Additionally, the wall thickness around the vent slot has been significantly increased, enhancing its capacity to withstand contact forces and consequently reducing stress in the upper fillet region of the baffle.

Table 5 Parameter optimization results at step 958

Parameter	Initial value/mm	Optimized value/mm	Change rate/%
d_1	1.25	1.52	+21.6
d_2	2.10	3.93	+87.1
R_1	2.00	3.50	+75.0
R_2	5.20	2.38	−54.2
R_3	1.00	2.58	+158.0
R_4	4.00	2.66	−33.5
R_5	0.50	0.96	+92.0
R_6	2.00	1.47	−26.5
l	4.44	4.02	−9.5

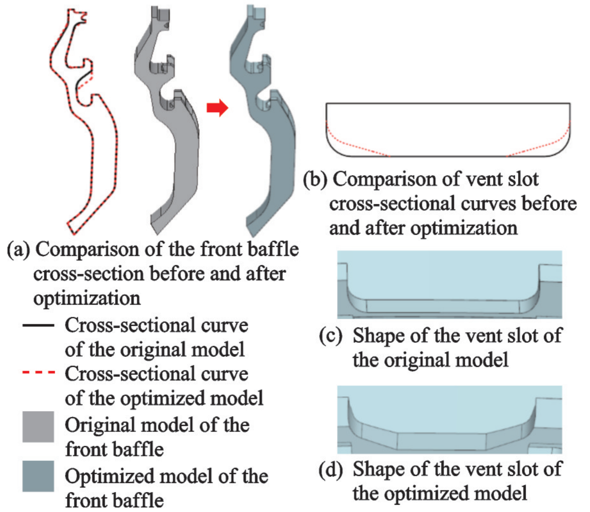

Fig.17 Comparison of original and optimized geometric models

Fig.18 presents a comparative analysis of the local stress contours of the baffle before and after optimization under the same scale. As shown in Fig.18, the stress in region A is significantly reduced after optimization. In combination with Table 5, it can be seen that the increase in wall thickness d_1 results in a thicker section in region A, leading to a notable improvement in stress in this area. In the ventilation slot region B, the slower transition of the slot geometry contributes to a substantial reduction in stress compared to the pre-optimized condition. The increase in wall thickness d_2 makes the stress distribution in region C more uniform than before optimization. Since the other parameters in regions C and D do not change significantly, their stress levels do not show a marked decrease. In summary, the stress in regions A and B of the baffle is clearly improved after optimization, and the stress distribution in region C becomes more uniform.

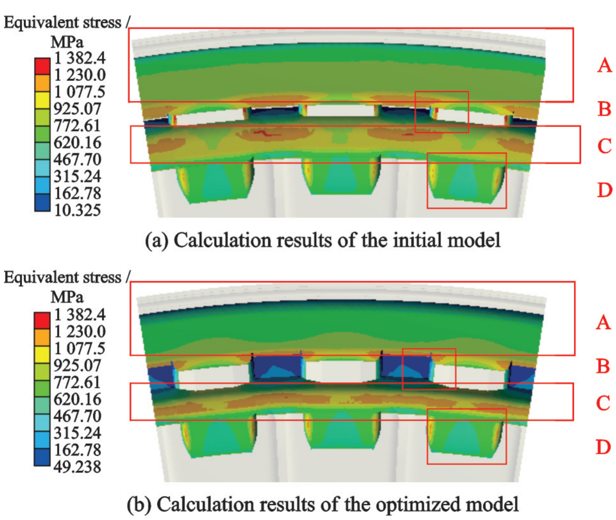

Fig.18 Comparison of local stress contours of the baffle before and after optimization

In this study, the particle swarm optimization (PSO) algorithm from the Zhizhou software and the multi-island genetic algorithm (MIGA) from the Isight optimization software are used to optimize the baffle, aiming to further compare and analyze the optimization performance of the SMA algorithm. To ensure the same number of evaluations during the optimization process, the population size of PSO is set to 20 with 50 iterations, while for MIGA, the population size, the number of islands, and the iteration count are all set to 10. The convergence curves of the three algorithms are shown in Fig.19.

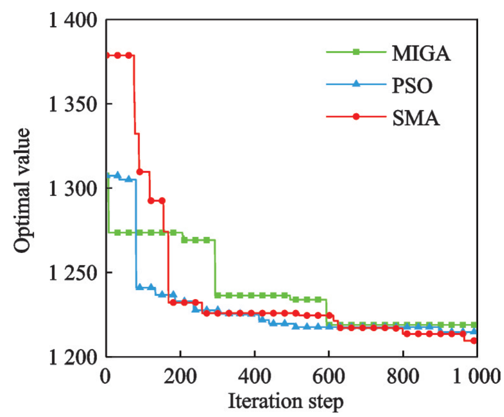

Fig.19 Convergence curves of the three algorithms

MIGA converges at around 600 iterations, demonstrating the fastest convergence among the three algorithms; however, it yields the poorest optimization result, indicating that MIGA tends to fall into local optima. The PSO algorithm converges at approximately 900 iterations, with a convergence speed slightly better than that of SMA, but its final optimization outcome is marginally inferior to that of SMA. The SMA algorithm converges at about 950 iterations. Although its convergence speed is the slowest among the three algorithms, it achieves the best optimization result, suggesting that SMA slightly outperforms the other two algorithms in terms of global search capability.

The final optimization results of the three algorithms are shown in Table 6. The optimized result obtained by MIGA is 1 255.3 MPa, that by PSO is 1 254.4 MPa, and that by SMA is 1 235.4 MPa. Using the optimization objective as the evaluation criterion, the SMA algorithm achieves the best optimization performance among the three algorithms.

Table 6 Performance of equivalent stress comparison between MIGA, PSO, and SMA

Algorithm	Equivalent stress of the initial mode/MPa	Equivalent stress of the optimized model/MPa	Change rate/%
MIGA	1 382.4	1 255.3	−9.2
PSO	1 382.4	1 254.4	−9.3
SMA	1 382.4	1 235.4	−10.6

As shown in Fig.20, a correlation analysis is conducted on the optimization parameters of the baffle, where red indicates a positive correlation and blue indicates a negative correlation. It can be seen from Fig.18 that parameters l, R_3 and R_2 have a relatively large impact on the stress. l is the vent slot shape control parameter. The maximum stress of the original baffle model occurs at the fillet of the vent slot, so this parameter directly affects the distribution of maximum stress. R_3 and R_2 jointly control the size of the fillet above the baffle's vent slot. The stress in this fillet area of the original model is also relatively high, so R_3 and R_2 also have a significant impact on the maximum stress of the baffle.

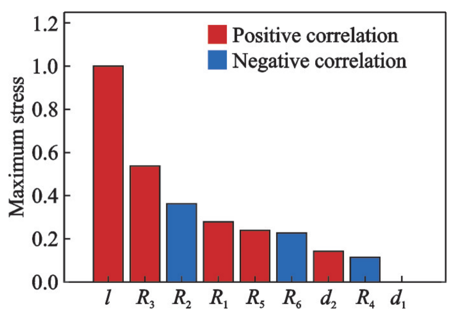

Fig.20 Parameter correlation analysis

5 Conclusions

This study addresses the issue of excessive local stress in the baffle of a high-pressure turbine disc in an aero-engine by conducting a structural design optimization of the component. Based on a finite element analysis incorporating simplified frictional contact conditions for the baffle, an integrated design optimization workflow is established using the self-developed Zhizhou software in combination with UG and Workbench. SMA is incorporated to perform the structural optimization. The following conclusions are drawn.

(1) Based on the calculation results of the high-pressure turbine sub-model, the contact force is used to replace the contact relationship between the sealing disk and the turbine disk, reducing the number of nonlinear contact pairs. With the simplified calculation method, the relative errors of the maximum equivalent stress before and after optimization are 0.3% and 0.06%, respectively; the calculation time is reduced from about 16 min to about 12 min, and the calculation efficiency is improved by 25%. These results verify the feasibility and effectiveness of the simplification method.

(2) The maximum equivalent stress of the optimized configuration is reduced to 1 235.4 MPa, representing a 10.6% decrease compared to the original model's value of 1 382.4 MPa. Further, the axial reaction force at the tenon contact interface reaches 4 330.6 N, corresponding to a 4.0% increase from the initial value of 4 158.9 N. This variation remains well within the prescribed constraint of 12%.

(3) The optimized design effectively reduces the maximum equivalent stress of the baffle, which verifies that the self-developed Zhizhou software has important value in solving practical engineering problems, and also confirms the effectiveness of the SMA algorithm in optimization.

References

[1] WANG Qingping. Research on the technology of sealing disk-baffle integrated structure design and optimization[D]. Nanjing: Nanjing University of Aeronautics and Astronautics, 2014. (in Chinese)

[2] CHEN Zhiying, ZHOU Ping, LIU Yong. Multi-objective collaborative robust optimization for turbine ro-

tor radial deformation[J]. Journal of Aerospace Power, 2018, 33(7): 1537-1543.(in Chinese)

[3] YANG Mujin, LU Songbing, YANG Dabing, et al. Fracture analysis of turbine rotor blades in an aircraft engine[J]. Journal of Aerospace Power, 2025, 40(12): 132-140. (in Chinese)

[4] MENG Qingdi, WANG Xinge, HAN Huiling. Calculating research on the centrifugal stress of aero-engine boltless retainer[J]. Aircraft Design, 2010, 30(4): 45-48. (in Chinese)

[5] LUAN Yongxian, LUO Guihuo. Analysis of contact pressure between boltless baffle and blade[J]. Journal of Aerospace Power, 2007, 22(9): 1550-1553. (in Chinese)

[6] ZENG Zhaohui, PI Zizi, LIU Yang, et al. Application of ANSYS sub-modeling for gas turbine rear cooling plate optimization[J]. Machinery, 2017, 44(7): 54-57. (in Chinese)

[7] SONG Yang, LI Yuwei, CHENG Ronghui, et al. Turbine disk baffle structure shape optimization method based on mesh deformation[J]. Journal of Thermal Science and Technology, 2023, 22(3): 300-306. (in Chinese)

[8] ZHU Jihong, HAN Jiacheng, GU Xiaojun, et al. Advances and challenges in cross-domain vehicle structures and morphing configuration design technologies[J]. Acta Aeronautica et Astronautica Sinica, 2025, 46(18): 275-306. (in Chinese)

[9] YANG Minchao, SUN Suya. Structural optimization of turbine tenon/mortise[J]. Journal of Aerospace Power, 2010, 25(8): 1876-1882. (in Chinese)

[10] ZHANG Xianxiang, WANG Dan, ZHANG Weihong. Development of optimization design system for aero-engine turbine stator[J]. Science Technology and Engineering, 2010, 10(7): 1710-1716. (in Chinese)

[11] SIVASHANMUGAM V K, ARABNIA M, GHALY W. Aero-structural optimization of an axial turbine stage in three-dimensional flow[J]. Turbomachinery, Parts A, B, and C, 2010(7): 967-980.

[12] SONG Dandan. Improved whale optimization algorithm and automatic structural optimization design of turbine disk[D]. Xiamen: Xiamen University, 2022. (in Chinese)

[13] FAN Jiang, ZENG Weiwei, WANG Rongqiao, et al. Optimization design of the turbine blade shroud based on iSIGHT software[J]. Journal of Aerospace Power, 2011, 26(4): 745-751. (in Chinese)

[14] SHANGGUAN Ronghai, HAO Yanhua, HUANG Zhijian. Structural optimization design of turbine blade with special-shroud[J]. Journal of Aerospace Power, 2018, 33(2): 313-319. (in Chinese)

[15] HAN Zimeng. Research on the improvement and application of slime mould algorithm[D]. Xi'an: Xi'an University of Technology, 2024. (in Chinese)

[16] AECC Commercial Aircraft Engine Co., Ltd. Advanced aero-engine materials and applications[EB/OL]. (2024-12-02). https://www.aecc.cn/aecc/zycp/xjkysshptrj/2024120222065332105/index.html. (in Chinese)

[17] MIRJALILI S, LEWIS A. The whale optimization algorithm[J]. Advances in Engineering Software, 2016, 95: 51-67.

[18] YAN Qunmin, MA Ruiqing, MA Yongxiang, et al. Adaptive simulated annealing particle swarm optimization algorithm[J]. Journal of Xidian University, 2021, 48(4): 120-127. (in Chinese)

[19] SONG C X, KAWAI R. Monte Carlo and variance reduction methods for structural reliability analysis: A comprehensive review[J]. Probabilistic Engineering Mechanics, 2023, 73: 103479.

[20] MEE R W. Introduction to full factorial designs with two-level factors[M]//A Comprehensive Guide to Factorial Two-Level Experimentation. New York, USA: Springer New York, 2009: 3-26.

[21] GUIDO R, FERRISI S, LOFARO D, et al. An overview on the advancements of support vector machine models in healthcare applications: A review[J]. Information, 2024, 15(4): 235.

[22] ZHOU J H, QIAN S T, HAN T, et al. Error prediction for machining thin-walled blade with Kriging model[J]. Results in Engineering, 2025, 26: 104645.

[23] GAO Shuai, YANG Zhanhai. Multi-strategy improved slime mold algorithm[J]. Journal of Yan'an University (Natural Science Edition), 2024, 43(3): 102-108,115. (in Chinese)

[24] LI S M, CHEN H L, WANG M J, et al. Slime mould algorithm: A new method for stochastic optimization[J]. Future Generation Computer Systems, 2020, 111: 300-323.

[25] SUN Hongyao. Research on sub-model technology of typical structure of turbine rotor[D]. Quanzhou: Huaqiao University, 2021. (in Chinese)

[26] SUN Haihe, QIN Shiyong, PANG Yanlong, et al. Transient thermo-mechanical coupling response analysis for boltless baffle of turbine rotor[J]. Gas Turbine Experiment and Research, 2020, 33(2): 44-47. (in Chinese)

Acknowledgements This work was supported in part by the National Natural Science Foundation of China (No. 52475285), the Natural Science Foundation of Fujian Province, China (No. 2025J09012), and Fundamental Research Funds for the Central Universities (No.20720240062).

Authors

The first author Mr. **PEI Ben** received his Bachelor degree on engineering from Xiamen University in 2024, and has been pursuing a Master's degree in aero-engine engineering at Xiamen University since September 2024. His research direction is multidisciplinary design optimization.

The corresponding author Dr. **YAN Cheng** received his Bachelor's degree and Doctor's degree from Beihang University in 2014 and 2019, respectively. Since 2019, he has been working at School of Aerospace Engineering, Xiamen University, where he currently holds the position of associate professor. He has long been engaged in research on aero-engine structural strength, structural topology optimization design, and multidisciplinary design optimization.

Author contributions Mr. **PEI Ben** was responsible for the main research work and the writing. Dr. **LIU Yiyuan** provided a high-pressure turbine model of a certain engine and related technical guidance. Mr. **CHEN Yalong** provided guidance on the finite element analysis in the paper. Dr. **TENG Da** provided guidance on the introduction of the algorithm in the paper. Mr. **HOU Naixian** was in charge of the research design and data analysis. Mr. **MI Dong** participated in the discussion of related research and gave suggestions on writing the background section. Dr. **YAN Cheng** offered guidance on the research work and writing of the paper. All authors commented on the draft manuscript and approved the final version for submission.

Competing interests The authors declare no competing interests.

(Production Editor: ZHANG Bei)

基于智周软件黏菌算法的涡轮挡板结构设计优化

裴 奔[1]，刘艺苑[2]，陈亚龙[2,3]，腾 达[1]，侯乃先[2]，米 栋[4]，闫 成[1]

(1.厦门大学航空航天学院,厦门 361102,中国; 2.中国航发商用航空发动机有限责任公司,上海 200241,中国; 3.华东理工大学机械与动力工程学院,上海 200237,中国; 4.中国航发湖南动力机械研究所,株洲 412002,中国)

摘要:挡板作为涡轮转子的关键组成部分,对发动机的安全可靠运行至关重要。针对某航空发动机高压涡轮盘挡板局部应力过大的问题,基于自研的国产智周软件,集成黏菌算法(Slime mould algorithm, SMA),开展了挡板结构设计优化研究。智周软件依托先进的算法和完备的仿真软件接口,能够充分挖掘结构设计潜力,实现结构性能的提升。SMA优化算法采用正反馈机制与自适应策略,通过引入适应度权重和振荡因子,模拟黏菌的振荡收缩行为,动态调整搜索方向和速度,有效平衡局部探索与全局寻优。在挡板结构设计优化中,首先构建扇区子模型,采用力载荷等效的方法对接触模型进行简化,以提高计算效率;其次,根据挡板几何特征、应力响应及边界约束分析,建立挡板参数化模型,并确定关键参数变化范围;然后,以降低最大等效应力为目标,以接触面的轴向支反力为约束,建立挡板优化数学模型;最后,基于智周软件构建联合Unigraphics(UG)和Workbench的设计优化流程,并集成SMA算法开展挡板结构设计优化。优化后,挡板最大等效应力由1 382.4 MPa降至1 235.4 MPa,降低了10.6%,轴向支反力由4 158.9 N变化至4 330.6 N,变化约4.0%,满足变化范围在12%以内的约束,验证了SMA算法在挡板结构设计优化中的有效性,也证实了智周软件在实际工程问题中具有重要价值。

关键词:高压涡轮;挡板;智周软件;黏菌算法;结构优化

研究亮点

1.基于国产自研的智周软件集成黏菌算法开展了挡板结构设计优化,体现了国产软件的开发与应用能力。

2.建立了挡板扇形子模型,并通过力载荷等效方式简化接触模型,显著提高了计算效率。优化后最大等效应力从1 382.4 MPa降至1 235.4 MPa(降幅10.6%),轴向支反力增幅仅4.0%,满足不超过12%的约束条件,验证了优化方法的有效性。

3.基于智周软件、UG和Workbench构建集成优化工作流,展示了多软件协同解决复杂工程问题的能力,验证了SMA算法在结构优化中的有效性,证明了智周软件在实际工程中的应用价值。